Journal of Solid Mechanics Vol. 13, No. 2 (2021) pp. 186-201
DOI: 10.22034/jsm.2020.1907521.1637

Response of Two-Temperature on the Energy Ratios at Elastic-Piezo-thermoelastic Interface

R. Kumar *, P. Sharma

Department of Mathematics, Kurukshetra University, Kurukshetra 136119, Haryana, India

Received 3 March 2021; accepted 30 April 2021

ABSTRACT

In the present investigation the reflection and transmission phenomenon of plane waves between two half spaces elastic and orthotropic piezo-thermoelastic with two-temperature theory is discussed. A piezo-thermoelastic solid half space is assumed to be loaded with an elastic half space. Due to the phenomenon, four qausi waves are obtained; Quasi longitudinal (QP) wave, Quasi Transverse (QS) wave, Quasi Thermal (QT) wave and Electric Potential wave (EP). It is found that the amplitude ratios of various reflected and refracted waves are functions of angle of incidence, frequency of incident wave and are influenced by the piezo-thermo-elastic properties of media. The energy ratios are computed numerically using amplitude ratios for a particular model of graphite and cadmium selenide (CdSe). The variations of energy ratios with angle of incidence are shown graphically depicting the effect of two-temperature. The conservation of energy across the interface is justified. A particular case of interest is also deduced from the present investigation.

Keywords : Reflection; Piezo-thermo-elastic; Energy ratios; Transmission; Orthotropic; Amplitude ratios.

1 INTRODUCTION

CHEN and Gurtin [1], and Chen et al. [2, 3], explored the heat conduction equation for the two-temperature theory of thermoelasticity involving conductive temperature and thermodynamic temperature. Sharma and Marin [4] studied the effect of distinct conductive and thermodynamic temperatures on the reflection of plane waves in micropolar elastic half-space. Kumar et al. [5] studied the propagation of plane waves in an anisotropic thermoelastic medium with void and two-temperature in the context of three phase lag theory of thermoelasticity. Mindlin [6] derived governing equations of a thermo-piezoelectric material. Nowacki [7, 8] examined the physical laws for the thermo-piezoelectric material. Due to piezoelectricity being the base of the modern engineering practice in various technologies like frequency control, signal processing, sound and ultrasound microphones and speakers, ultrasonic imaging, hydrophones, actuators and motors based on the converse effect, detection of pressure variations in the form of sound etc. different academicians have been exploring and solving different problems. Few of them are Vashishth and Sukhija [9-11], Kumar and Sharma [12], Marin and Ochsner [13], Sharma [14], Kumar and Sharma [15]. Youssef and Bassiouny [16] proposed the generalised two temperature theory of thermoelasticity to solve the boundary value problems of one dimensional piezo-thermoelastic half-space with heating its boundary

*Corresponding author. Tel.: +91 94161 20992.
E-mail address: rajneesh_kuk@rediffmail.com (R.Kumar)

with different types of heating. Ezzat et al. [17] formulated the theory of two temperature theory of thermoelasticity for piezoelectric/piezomagnetic materials.

The investigation of existing model involving ES and OPS with two temperature parameter has been taken into account with growing interest under the impact of various physical properties. An orthotropic piezothermoelastic half-space (OPS) loaded with elastic half-space (ES) is considered. Amplitude ratios are used to determine the energy ratios. These ratios are derived with suitable boundary conditions. The impact of two-temperature parameter on these ratios is shown graphically.

2 BASIC EQUATIONS

Following Kumar et al. [5] and Kumar & Sharma [15], the governing equations for a homogeneous, anisotropic, thermally conducting, piezoelectric elastic medium are as follows:

Constitutive equations

$$\sigma_{ij} = c_{ijkl}\,\varepsilon_{kl} - e_{ijk} E_k - \alpha_{ij} T\ , \tag{1}$$

$$-q_{i,i} = \rho T_0 \dot{S}, \tag{2}$$

$$\rho S = \alpha_{ij}\varepsilon_{ij} + \tau_i E_i + rT\ , \tag{3}$$

$$D_i = \xi_{ij} E_j + e_{ijk}\varepsilon_{jk} + \tau_i T\ , \tag{4}$$

$$E_i = -\phi_{,i}\ , (i, j, k, l = 1,2,3) \tag{5}$$

Equations of motion

$$\sigma_{ij,j} + \rho(F_i - \ddot{u}_i) = 0, \tag{6}$$

Equation of heat conduction

$$-K_{ij}\ \varphi_{,j} = \left(1 + \tau_0 \frac{\partial}{\partial t}\right) q_i\ , \tag{7}$$

Such that $\varphi - T = a_{ij}\varphi_{,ij}$.

Gauss equation

$$D_{i,i} = 0. \tag{8}$$

For ES, following Achenbach [32], the relations are

$$\sigma^e_{ij} = 2\mu^e u^e_{i,j} + \lambda^e u^e_{k,k}\delta_{ij}\ , \quad (i, j, k, l = 1,2,3) \tag{9}$$

$$\mu^e u^e_{i,jj} + (\lambda^e + \mu^e) u^e_{i,ij} - \rho^e \ddot{u}^e_i = 0, \left(i, j = 1,2,3\right) \tag{10}$$

where

E_i - electric field intensity,

D_i - electric displacement,

ϕ - electric potential,

τ_i - pyroelectric constants,
T - absolute temperature,
φ - conductive temperature,
a_{ij} - two-temperature parameters,
e_{ijk}, ξ_{ij} - piezo-thermal coupling tensors, and other symbols are well defined. Superscript 'e' represents elastic half space.

3 STATEMENTS OF THE PROBLEM AND SOLUTION

Consider an OPS, in welded contact with an elastic half space (ES) (Fig. 1and Fig.2) in order that the OPS occupies the region $x_3 > 0$, and the ES occupies region $x_3 < 0$ and $x_3 = 0$ is the boundary interface. We take plane waves in the $x_1 - x_3$ plane with wave-front parallel to the x_2 axis.

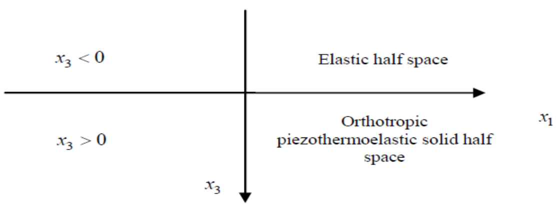

Fig.1
Geometry of the problem.

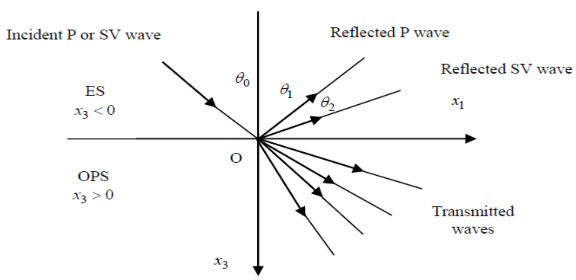

Fig.2
Reflection and transmission of plane wave.

For two-dimensional problem, the displacement vectors are taken as $\mathbf{u} = (u_1, 0, u_3)$ and $\mathbf{u}^{\boldsymbol{e}} = (u_1^e, 0, u_3^e)$. Following Tzou and Bao [18], the constitutive relations in $x_1 - x_3$ plane are

$$\sigma_{11} = c_{11}\varepsilon_1 + c_{13}\varepsilon_3 - e_{31}E_3 - \alpha_{11}T, \quad (11a)$$

$$\sigma_{33} = c_{13}\varepsilon_1 + c_{33}\varepsilon_3 - e_{33}E_3 - \alpha_{33}T, \quad (11b)$$

$$\sigma_{13} = 2c_{55}\varepsilon_5 - e_{15}E_1, \quad (11c)$$

$$D_1 = \xi_{11}E_1 + 2e_{15}\varepsilon_5, \quad (11d)$$

$$D_3 = \xi_{33}E_3 + e_{31}\varepsilon_1 + e_{33}\varepsilon_3 + \tau_3 T, \quad (11e)$$

$$E_1 = -\phi_{,1}, \quad (11f)$$

$$E_3 = -\phi_{,3}, \quad (11g)$$

Similar relations for ES are

$$\sigma_{11}^{e}=\mu^{e}\,u_{1,1}^{e}+\lambda^{e}\,(u_{1,1}^{e}+u_{3,3}^{e}),\tag{12a}$$

$$\sigma_{33}^{e}=\mu^{e}\,u_{3,3}^{e}+\lambda^{e}\,(u_{1,1}^{e}+u_{3,3}^{e}),\tag{12b}$$

$$\sigma_{13}^{e}=\mu^{e}\,(u_{3,1}^{e}+u_{1,3}^{e}).\tag{12c}$$

Putting (11a)-(11g) into the field Eqs. (6)-(8) in the absence of body forces, heat sources, yield

$$c_{11}\,u_{1,11}+c_{13}\,u_{3,13}+e_{31}\phi_{,31}+c_{55}(u_{1,33}+u_{3,13})-\alpha_{11}(\varphi-a_{11}\varphi_{,11}-a_{33}\varphi_{,33})_{,1}+e_{15}\phi_{,13}-\rho\ddot{u}_{1}=0,\tag{13a}$$

$$c_{55}(u_{1,31}+u_{3,11})+c_{13}\,u_{1,13}+c_{33}\,u_{3,33}-\alpha_{33}(\varphi-a_{11}\varphi_{,11}-a_{33}\varphi_{,33})_{,3}+e_{15}\phi_{,11}+e_{33}\phi_{,33}-\rho\ddot{u}_{3}=0,\tag{13b}$$

$$(K_{11}\varphi_{,11}+K_{33}\varphi_{,33})-\left(1+\tau_{0}\frac{\partial}{\partial t}\right)T_{0}(\alpha_{11}\,\dot{u}_{1,1}+\alpha_{33}\,\dot{u}_{3,3}-\tau_{3}\dot{\phi}_{,3}+r(\dot{\varphi}-a_{11}\dot{\varphi}_{,11}-a_{33}\dot{\varphi}_{,33}))=0,\tag{13c}$$

$$-\xi_{11}\phi_{,11}+e_{15}(u_{1,31}+u_{3,11})-\xi_{33}\phi_{,33}+e_{31}\,u_{1,31}+e_{33}\,u_{3,33}+\tau_{3}(\varphi-a_{11}\varphi_{,11}-a_{33}\varphi_{,33})_{,3}=0.\tag{13d}$$

and for ES are

$$\left(\lambda^{e}+\mu^{e}\right)(u_{1,11}^{e}+u_{3,13}^{e})+\mu^{e}u_{1,33}^{e}-\rho^{e}\ddot{u}_{1}^{e}=0,\tag{14a}$$

$$\left(\lambda^{e}+\mu^{e}\right)(u_{3,33}^{e}+u_{1,31}^{e})+\mu^{e}u_{3,11}^{e}-\rho^{e}\ddot{u}_{3}^{e}=0.\tag{14b}$$

Take the following dimensionless quantities:

$$\begin{gathered}\left(x_{1}',x_{3}',u_{1}',u_{3}',u_{1}^{e}{}',u_{3}^{e}{}'\right)=\frac{\omega_{1}}{c_{1}}\left(x_{1},x_{3},u_{1},u_{3},u_{1}^{e},u_{3}^{e}\right),\ \left(t',\tau_{0}'\right)=\omega_{1}\left(t,\tau_{0}\right),\left(T',\varphi'\right)=\frac{\alpha_{11}}{\rho c_{1}^{2}}\left(T,\varphi\right),\\ \phi'=\frac{\omega_{1}e_{31}\phi}{c_{1}\alpha_{11}T_{0}},\left(\sigma_{ij}',\sigma_{ij}^{e}{}'\right)=\frac{1}{\alpha_{11}T_{0}}\left(\sigma_{ij},\sigma_{ij}^{e}\right),(P',P^{e}{}')=\frac{1}{\alpha_{11}T_{0}c_{1}}(P,P^{e}),(a_{11}',a_{33}')=\frac{\omega_{1}^{2}}{c_{1}^{2}}(a_{11},a_{33}),\end{gathered}\tag{15}$$

where $c_{1}=\sqrt{\frac{c_{11}}{\rho}}$, $\omega_{1}=\frac{\rho C_{e}c_{1}^{2}}{K_{11}}$.

Invoking dimensionless Eqs. (15) in the system of Eqs. (13a) - (14b), with the removal of prime ('), leads to the following form

$$c_{11}\,u_{1,11}+(c_{13}+c_{55})\,u_{3,13}+c_{55}\,u_{1,33}+\frac{\alpha_{11}T_{0}}{e_{31}}(e_{31}+e_{15})\phi_{,13}-\rho c_{1}^{2}(\varphi-a_{11}\varphi_{,11}-a_{33}\varphi_{,33})_{,1}-\rho c_{1}^{2}\,\ddot{u}_{1}=0,\tag{16a}$$

$$(c_{55}+c_{13})\,u_{1,31}+c_{55}\,u_{3,11}+c_{33}\,u_{3,33}-\rho c_{1}^{2}\frac{\alpha_{33}}{\alpha_{11}}(\varphi-a_{11}\varphi_{,11}-a_{33}\varphi_{,33})_{,3}+\frac{\alpha_{11}T_{0}}{e_{31}}(e_{15}\phi_{,11}+e_{33}\phi_{,33})-\rho c_{1}^{2}\,\ddot{u}_{3}=0,\tag{16b}$$

$$\frac{\rho\omega_{1}}{\alpha_{11}}(K_{11}\varphi_{,11}+K_{33}\varphi_{,33})-\left(1+\tau_{0}\frac{\partial}{\partial t}\right)T_{0}(\alpha_{11}\,\dot{u}_{1,1}+\alpha_{33}\,\dot{u}_{3,3}-\tau_{3}\dot{\phi}_{,3}+r(\dot{\varphi}-a_{11}\dot{\varphi}_{,11}-a_{33}\dot{\varphi}_{,33}))=0,\tag{16c}$$

$$-\frac{\alpha_{11}T_0}{e_{31}}(\xi_{11}\phi_{,11}+\xi_{33}\phi_{,33})+e_{15}(\mathrm{u}_{1,31}+\mathrm{u}_{3,11})+e_{31}\,\mathrm{u}_{1,31}+e_{33}\,\mathrm{u}_{3,33}+\tau_3\frac{\rho c_1^{\,2}}{\alpha_{11}}(\varphi-a_{11}\varphi_{,11}-a_{33}\varphi_{,33})_{,3}=0, \tag{16d}$$

$$\left(\frac{\alpha^{e^2}-\beta^{e^2}}{c_1^2}\right)\left(\frac{\partial^2\mathrm{u}_1^e}{\partial x_1^{\,2}}+\frac{\partial^2\mathrm{u}_3^e}{\partial x_3\partial x_1}\right)+\frac{\beta^{e^2}}{c_1^2}\left(\frac{\partial^2\mathrm{u}_1^e}{\partial x_1^{\,2}}+\frac{\partial^2\mathrm{u}_1^e}{\partial x_3^{\,2}}\right)=\frac{\partial^2\mathrm{u}_1^e}{\partial t^2}, \tag{17a}$$

$$\left(\frac{\alpha^{e^2}-\beta^{e^2}}{c_1^2}\right)\left(\frac{\partial^2\mathrm{u}_1^e}{\partial x_3\partial x_1}+\frac{\partial^2\mathrm{u}_3^e}{\partial x_3^{\,2}}\right)+\frac{\beta^{e^2}}{c_1^2}\left(\frac{\partial^2\mathrm{u}_3^e}{\partial x_1^{\,2}}+\frac{\partial^2\mathrm{u}_3^e}{\partial x_3^{\,2}}\right)=\frac{\partial^2\mathrm{u}_3^e}{\partial t^2}, \tag{17b}$$

where $\alpha^e=\sqrt{\frac{\lambda^e+2\mu^e}{\rho^e}}$, $\beta^e=\sqrt{\frac{\mu^e}{\rho^e}}$ are velocities of longitudinal and transverse waves respectively. The displacement components are

$$\mathrm{u}_1^e=\frac{\partial\phi^e}{\partial x_1}-\frac{\partial\psi^e}{\partial x_3},\ \mathrm{u}_3^e=\frac{\partial\phi^e}{\partial x_3}+\frac{\partial\psi^e}{\partial x_1}, \tag{18}$$

where ϕ^e and ψ^e satisfies

$$\nabla^2\phi^e=\frac{\ddot{\phi}^e}{\alpha'^2},\ \nabla^2\psi^e=\frac{\ddot{\psi}^e}{\beta'^2},\alpha'=\frac{\alpha^e}{c_1},\ \beta'=\frac{\beta^e}{c_1}. \tag{19}$$

For plane wave solution, we take

$$(\mathrm{u}_1,\mathrm{u}_3,\phi,\varphi)=(U,A,B,C)\exp\left[i\,\omega\left(-\frac{x_1}{c}-qx_3+t\right)\right], \tag{20}$$

where

ω - Circular frequency,

q - Slowness parameter,

c - Apparent phase velocity,

U, A, B and C - Amplitude vectors.

Eqs. (16a) - (16b), along with Eq. (20), lead to a system

$$\boldsymbol{VS}=0, \tag{21}$$

where

$$\boldsymbol{V}=\begin{bmatrix} c_{55}q^2+x_{11} & x_{12}q & x_{13}q & x_{15}q^2+x_{14} \\ x_{12}q & c_{33}q^2+x_{17} & x_{18}+x_{19}q^2 & x_{21}q^3+x_{20}q \\ x_{22} & x_{23}q & x_{24}q & x_{30}q^2+x_{29} \\ x_{31}q & e_{33}q^2+x_{32} & x_{34}q^2+x_{33} & x_{36}q^3+x_{35}q \end{bmatrix} \tag{22}$$

and $\boldsymbol{S}=[U,A,B,C]^{tr}$. Here, superscript symbol " tr " represents transpose of the matrix. The symbols used in matrix $\boldsymbol{V}$ are mentioned in the Appendix A. To solve the system (21), we have

$$\det \boldsymbol{V} = 0. \tag{23}$$

Eq. (23) yields a characteristic equation in q. Solution of Eq. (23) determines the roots q_1, q_2, q_3 and q_4 with positive imaginary parts and q_5, q_6, q_7, q_8 with negative imaginary parts. The eigen values are arranged in descending order such that q_1, q_2 and q_3 corresponds to the propagating quasi P (qP) mode, quasi S (qS) mode, quasi T (qT) mode and q_4 corresponds to the electric potential component wave mode (eP) of wave propagation, respectively. For each q_i $(i = 1, 2, ..., 8)$, the corresponding eigen vectors U_i, A_i, B_i and C_i are

$$W_i = \frac{cof\,(V_{42})_{q_i}}{cof\,(V_{41})_{q_i}},\ \Phi_i = \frac{cof\,(V_{43})_{q_i}}{cof\,(V_{41})_{q_i}},\ \Theta_i = \frac{cof\,(V_{44})_{q_i}}{cof\,(V_{41})_{q_i}}, \tag{24}$$

where

$$W_i = \frac{A_i}{U_i},\ \Phi_i = \frac{B_i}{U_i},\ \Theta_i = \frac{C_i}{U_i}, \tag{25}$$

and $cof\,(V_{ij})_{q_i}$ denotes the cofactor of V_{ij} to the eigen value q_i. The formal expression for displacement, the electric potential and temperature becomes

$$(\mathrm{u}_1, \mathrm{u}_3, \phi, \varphi) = \sum_{i=1}^{8} (1, W_i, \Phi_i, \Theta_i) U_i \exp\left(i\omega\left(-\frac{x_1}{c} - q_i x_3 + t \right)\right), \tag{26}$$

The solution of ϕ^e and ψ^e can be expressed as:

$$\left.\begin{aligned} \phi^e &= A_0^e e^{\left[i\omega\left(\frac{-x_1 \sin\theta_0 - x_3 \cos\theta_0}{\alpha'} + t \right)\right]} + A_1^e e^{\left[i\omega\left(\frac{-x_1 \sin\theta_0 + x_3 \cos\theta_0}{\alpha'} + t \right)\right]}, \\ \psi^e &= B_0^e e^{\left[i\omega\left(\frac{-x_1 \sin\theta_0 - x_3 \cos\theta_0}{\beta'} + t \right)\right]} + B_1^e e^{\left[i\omega\left(\frac{-x_1 \sin\theta_0 + x_3 \cos\theta_0}{\beta'} + t \right)\right]}, \end{aligned}\right\} \tag{27}$$

where $A_0^e (B_0^e)$ - amplitudes of the incident P(or SV) wave and A_1^e, B_1^e - the amplitudes of reflected P wave and reflected SV wave, respectively.

4 REFLECTION AND TRANSMISSION COEFFICIENTS

4.1 Amplitude ratios

A plane wave (longitudinal or transverse), making an angle θ_0 with the x_3 axis is incident at the interface through the ES. This wave results in one reflected longitudinal wave (P wave) and one reflected transverse wave (SV wave) in the ES and four transmitted waves, represented by qP, qS, qT corresponds to the quasi-longitudinal, quasi-transverse, quasi-thermal and electric potential wave mode in the OPS. For OPS, the solution is:

$$\left.\begin{aligned} (\mathrm{u}_1, \mathrm{u}_3, \phi, \varphi) &= \sum_i (1, W_i, \Phi_i, \Theta_i) U_i \exp\left\{ i\omega\left(-\frac{x_1}{c} - q_i x_3 + t \right)\right\}, \\ (\sigma_{33}, \sigma_{31}, D_3) &= i\omega \sum_i (D_{1i}, D_{2i}, D_{6i}) U_i \exp\left\{ i\omega\left(-\frac{x_1}{c} - q_i x_3 + t \right)\right\}, \end{aligned}\right\} \tag{28}$$

where $c = \dfrac{V_0}{\sin\theta_0}$, $V_0 = \alpha'$ for incident P wave and $V_0 = \beta'$ for incident SV wave. The coefficients D_{1i}, D_{2i} and D_{6i} have been computed and are mentioned in Appendix B. The formal solution of wave in elastic medium is given by Eq. (26). The boundary conditions at the interface $x_3 = 0$ are as follows:

Continuity of normal stress

$$\sigma_{33} = \sigma_{33}^e, \tag{29a}$$

Continuity of the tangential stress

$$\sigma_{13} = \sigma_{13}^e, \tag{29b}$$

Continuity of tangential displacement

$$\mathrm{u}_1 = \mathrm{u}_1^e, \tag{29c}$$

Continuity of normal displacement

$$\mathrm{u}_3 = \mathrm{u}_3^e, \tag{29d}$$

Thermally insulated boundary

$$\frac{\partial T}{\partial x_3} = 0, \tag{29e}$$

Vanishing of electric displacement

$$D_3 = 0, \tag{29f}$$

Eqs. (16a) - (19), (26) - (27) and boundary conditions (29a) - (29f) determine

$$\boldsymbol{AX} = \boldsymbol{B}, \tag{30}$$

where

$$A = \begin{pmatrix} D_{11} & D_{12} & D_{13} & D_{14} & D_{15} & D_{16} \\ D_{21} & D_{22} & D_{23} & D_{24} & D_{25} & D_{26} \\ D_{31} & D_{32} & D_{33} & D_{34} & D_{35} & D_{36} \\ D_{41} & D_{42} & D_{43} & D_{44} & D_{45} & D_{46} \\ D_{51} & D_{52} & D_{53} & D_{54} & 0 & 0 \\ D_{61} & D_{62} & D_{63} & D_{64} & 0 & 0 \end{pmatrix},$$

$$\boldsymbol{X} = \left[X_1, X_2, X_3, X_4, X_5^e, X_6^e\right]^{tr}, \; \boldsymbol{B} = \left[N_1, N_2, N_3, N_4, 0, 0\right]^{r}.$$

The elements of 6×6 matrix $\boldsymbol{A}$ and notations used in $\boldsymbol{X}$ and $\boldsymbol{B}$ are given in the Appendix B. After solving the system (30), the transmitted and the reflected amplitude ratios are obtained.

4.2 Energy ratios

The distribution of energy between different reflected and transmitted waves at the interface $x_3 = 0$, across a surface element of unit area is considered. Following Vashishth and Sukhija [20], the normal acoustic flux P in OPS is

$$P = -\mathrm{Re}\left(\sigma_{31}\dot{\bar{u}}_1 + \sigma_{33}\dot{\bar{u}}_3 - \phi\dot{\bar{D}}_3 + K_{33}\bar{T}_{,3}\frac{T}{T_0}\right) \tag{31}$$

and, in ES is

$$P^e = -\mathrm{Re}(\sigma_{31}^e\dot{\bar{u}}_1^e + \sigma_{33}^e\dot{\bar{u}}_3^e). \tag{32}$$

The time average of P over a period denoted by $< P >$ represents the average energy transmission per unit surface area per unit time. The average energy flux for

The incident waves

$$\langle P_{IP}^e \rangle = \frac{1}{2\alpha'}\omega^4\rho^e c_1^2 \,\mathrm{Re}(\cos\theta_0)\left|A_0^e\right|^2, \quad \langle P_{IS}^e \rangle = \frac{1}{2\beta'}\omega^4\rho^e c_1^2 \,\mathrm{Re}(\cos\theta_0)\left|B_0^e\right|^2, \tag{33}$$

The reflected waves

$$\langle P_{RP} \rangle = -\frac{1}{2\alpha'}\omega^4\rho^e c_1^2 \,\mathrm{Re}\left(\cos\theta_1\right)\left|A_1^e\right|^2, \quad \langle P_{RS}^e \rangle = -\frac{1}{2\beta'}\omega^4\rho^e c_1^2 \,\mathrm{Re}\left(\cos\theta_2\right)\left|B_1^e\right|^2, \tag{34}$$

The transmitted waves

$$\langle P_s \rangle = \frac{1}{2}\omega^2 \,\mathrm{Re}\left(D_{2s} + D_{1s}\bar{W}_s + \bar{D}_{6s}\Phi_s + \frac{i}{\omega}\frac{K_{33}}{T_0}\bar{D}_{5s}\left(t_{14} + t_{15}q_s^2\right)\Theta_s\right)\left|U_s\right|^2, \left(s = 1,2,3,4\right). \tag{35}$$

The energy ratios of the reflected and transmitted waves for incident

(i) P wave

$$E_{RP} = \frac{\langle P_{RP}^e \rangle}{\langle P_{IP}^e \rangle}, \; E_{RS} = \frac{\langle P_{RS}^e \rangle}{\langle P_{IP}^e \rangle}, \; ES_s = \frac{\langle P_s \rangle}{\langle P_{IP}^e \rangle}, \left(s = 1,2,3,4\right). \tag{36}$$

(ii) SV wave

$$E_{RP} = \frac{\langle P_{RP}^e \rangle}{\langle P_{IS}^e \rangle}, \; E_{RS} = \frac{\langle P_{RS}^e \rangle}{\langle P_{IS}^e \rangle}, \; ES_s = \frac{\langle P_s \rangle}{\langle P_{IS}^e \rangle}, \left(s = 1,2,3,4\right). \tag{37}$$

The interaction energy ratios for the both cases, which account for the interaction between different fields and displacements corresponding to transmitted waves are; $E_{st} = \frac{\langle P_{st} \rangle}{\langle P_{IP}^e \rangle}$ for incident P wave and $E_{st} = \frac{\langle P_{st} \rangle}{\langle P_{IS}^e \rangle}$ for incident SV wave where

$$\langle P_{st} \rangle = \frac{1}{2}\omega^2 \,\mathrm{Re}\left(D_{2s}U_s\bar{U}_t + D_{1s}\bar{W}_tU_s\bar{U}_t + \bar{D}_{6s}\Phi_tU_t\bar{U}_s + \frac{i}{\omega}\frac{K_{33}}{T_0}\left(t_{14} + t_{15}q_s^2\right)\bar{D}_{5s}\Theta_s\bar{U}_sU_t\right), \left(s = 1,2,3,4\right). \tag{38}$$

The energy is conserved if

$$\sum_{s=1}^{4} ES_s + E_{\text{int}} + E_{RP} + E_{RS} = 1, \tag{39}$$

where $E_{\text{int}} = \sum_{\substack{s,t=1 \\ s \neq t}}^{4} E_{st}$ is the resultant interaction energy between the transmitted waves.

Unique case

If we put $a_{11} = a_{33} = 0,$ in system of Eqs. (13) then the matrix $\boldsymbol{V}$ reduces to

$$\boldsymbol{V} = \begin{bmatrix} c_{55}q^2 + x_{11} & x_{12}q & x_{13}q & 0 \\ x_{12}q & c_{33}q^2 + x_{17} & x_{18} + x_{19}q^2 & 0 \\ x_{22} & x_{23}q & x_{24}q & x_{26}q^2 + x_{25} \\ x_{31}q & e_{33}q^2 + x_{32} & x_{34}q^2 + x_{33} & 0 \end{bmatrix},$$

and, for the non-trivial solution $|\boldsymbol{V}| = 0,$ yielding a characteristic equation

$$m_{11}q^8 + m_{12}q^6 + m_{13}q^4 + m_{14}q^2 + m_{15} = 0,$$

where the notations $m_{1i}, (i = 1,2,3,4,5)$ are mentioned in the Appendix A. Solving the characteristic equation we obtain the unknown amplitude of the respective waves and hence, energy ratios at the interface of ES and OPS can be obtained verifying the law of conservation of energy.

5 RESULTS AND DISCUSSION

The amplitude ratios and energy ratios for different waves are computed numerically with the help of softwares Matlab 9.0 and Origin 6.1. Graphs of energy ratios of waves are shown depicting the effect of two-temperature parameter. Further, law of conservation of energy is verified. Following Vashishth and Sukhija [10], the numerical values of cadmium selenide (CdSe) have been taken. Elastic constants (in units of GPa) are $c_{11} = 74.1, c_{13} = 39.3,$ $c_{33} = 83.6, c_{55} = 15.1,$ thermo-elastic coupling constants $(10^5\, NK^{-1}m^{-2})$ are $\alpha_{11} = 6.21,\ \alpha_{33} = 5.51,$ electric permittivity constants $(10^{-11} C^2N^{-1}m^{-2})$ are $\xi_{11} = 8.26,\ \ \xi_{33} = 9.03,$ thermal conductivity constants $(Wm^{-1}K^{-1})$ are $K_{11} = 9,\ K_{33} = 9,$ pyroelectric constant is $\tau_3 = -2.6 \times 10^{-6}\, Cm^{-2}K^{-1}.$ $e_{15} = 3,\ e_{31} = 35, e_{33} = 34$ are the piezoelectric constants $(10^{-3}\, Cm^{-2}).$ Numerical values for the remaining constants are $\rho = 5504\, Kgm^{-3}, a_{11} = 10^{-20},\ a_{33} = 2 \times 10^{-20}, T_0 = 298K,\ C_e = 260 JKg^{-1}K^{-1},\ \tau_0 = 2 \times 10^{-12} s,\ \ \omega = 2\pi \times 10^3 Hz.$ Following Bullen [19], the numerical data of graphite in elastic medium is given by $\alpha^e = 0.0011 \times 10^3 ms^{-1}, \rho^e = 2.65 \times 10^3 Kgm^{-3},\ \ \beta^e = 0.001 \times 10^3 ms^{-1}.$ In all the graphs, notations ▭, WTT, ▨, WOTT denote the energy ratio curves corresponding to orthotropic piezo-thermoelastic solid with two-temperature and orthotropic piezo-thermoelastic solid, respectively.

5.1 Incident P wave

From Figs. 3,4, it is clear that for both models i.e. WTT and WOTT, energy ratios of reflected and transmitted waves demonstrate the same behavior but a slight difference in magnitude values demonstrating very small impact of two-temperature parameters. For WTT and WOTT models, energy ratio of reflected QP wave (E_{RP}) exhibits an increasing trend with increase in the magnitude values for $0 \le \theta_0 \le 80^0$ and then monotonically decreases as angle of incidence increases. Energy ratio of reflected QS wave (E_{RS}) depicts the opposite behavior to E_{RP}. For a particular range of angle of incidence i.e. $0 \le \theta_0 \le 80^0$, it displays a decreasing trend and then increases with further changes in angle of incidence. In Fig. 5, due to activeness of two temperature parameters ES_1 propagates fluctuating with small change in values whereas for WOTT model, it exhibits constant behavior for $\theta_0 \le 60^0$ and then displays increasing-decreasing trend for $\theta_0 \ge 80^0$. In Fig. 6, a significant change in the magnitude values of ES_2 can be seen due to the effect of two-temperature parameters for θ_0 varying from 0 to 20^0. For a particular range of θ_0 i.e. 20^0 to 80^0, a slight increase in magnitude values is noticed gradually but for θ_0 greater than or equals to 80^0, it again demonstrates a decreasing trend. For WOTT, ES_2 possesses a constant behaviour irrespective of change in θ_0. It is clear from Fig. 7 that for WTT model, ES_3 *depicts* a continuous increasing trend and for WOTT, it shows a constant behaviour with slight difference in numerical values as θ_0 changes. In Fig. 8, ES_4 demonstrates a constant behaviour due to the presence of two-temperature effect. For WOTT model, ES_4 propagates in a constant manner for $\theta_0 \le 60^0$ and then decreases sharply for $60^0 \le \theta_0 \le 80^0$ and further tends to increase such that the magnitude value for $\theta_0 \le 60^0$ is approximately similar to the value obtained at $\theta_0 = 100^0$. It is clear from Fig. 9 that although the change in magnitude values of E_{int} *are* ominous but the behaviour of interaction energy remains the same in the presence of two-temperature parameters. It demonstrates the decreasing behaviour with the change in direction.

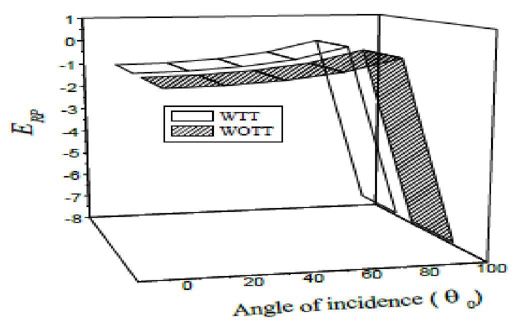

Fig.3
Profile of E_{RP} with θ_0.

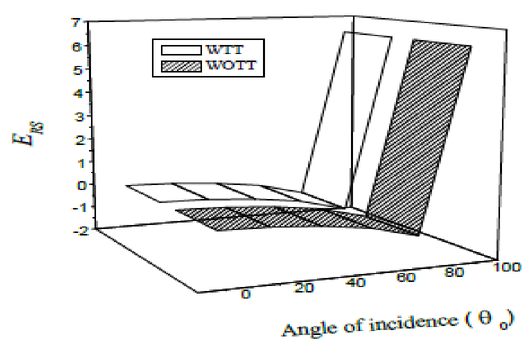

Fig.4
Profile of E_{RS} with θ_0.

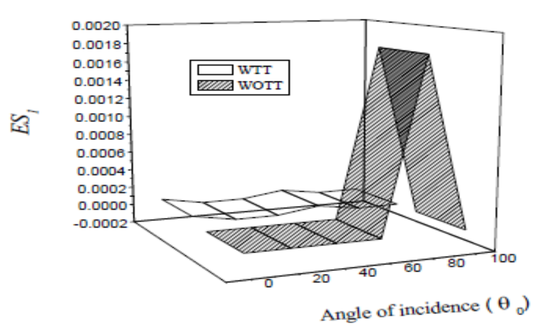

Fig.5
Profile of ES_1 with θ_0.

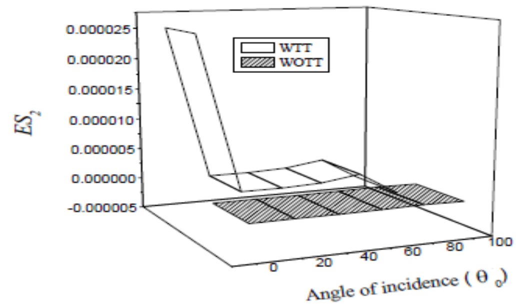

Fig.6
Profile of ES_2 with θ_0.

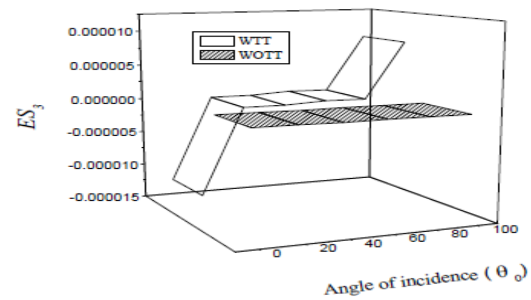

Fig.7
Profile of ES_3 with θ_0.

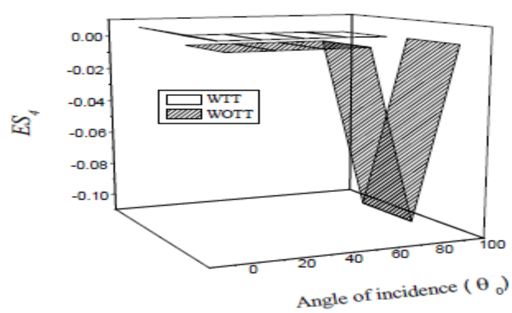

Fig.8
Profile of ES_4 with θ_0.

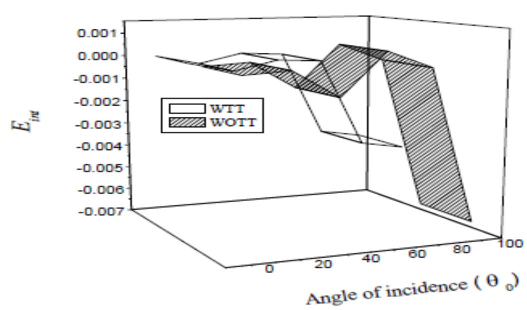

Fig.9
Profile of E_{int} with θ_0.

5.2 Incident SV wave

Figs. 10, 11 depict that E_{RP} *and* E_{RS} both display the similar behaviour in the presence/absence of two temperature parameters as angle of incidence varies. Initially, E_{RP} increases as θ_0 increases for $0 \le \theta_0 \le 20^0$ and for $\theta_0 \ge 20^0$, it possesses constant behaviour. E_{RS} displays the behaviour opposite to E_{RP} for both models but both behaves as a constant function for $\theta_0 \ge 20^0$. It is clear from Fig. 12 that for WTT model, ES_1 demonstrates a fluctuating behaviour with smaller variations in numerical values as direction of propagation changes. In the absence of two-temperature effect, ES_1 exhibits a monotonic increasing behaviour for θ_0 lies between 0 and 80^0 then decreases monotonically for further values of θ_0 . In Fig.13, ES_2 depicts an alternating behaviour for WTT as angle of incidence varies. Initially it increases for $0 \le \theta_0 \le 80^0$ and then decreases for $\theta_0 \ge 80^0$. In the absence of two-temperature effect, it shows a monotonic increasing trend with the change in direction of propagation. From Fig. 14, it is depicted that for WTT, ES_3 *increases* monotonically whereas for WOTT, it possesses constant behaviour with the small variations in magnitude values as θ_0 changes. In Fig. 15, ES_4 *demonstrates* a constant behaviour due to the presence of two-temperature effect. If two-temperature effect is neglected then ES_4 propagates in a constant manner for $\theta_0 \le 60^0$ and then decreases monotonically for $60^0 \le \theta_0 \le 80^0$ and for $\theta_0 \le 60^0$, it tends to increase monotonically. Fig. 16 displays that for $0 \le \theta_0 \le 40^0$ and in the presence of two-temperature effect E_{int} *shows* an alternating i.e. increasing/decreasing behaviour and then it propagates as a constant function for further values of angle of incidence. Similarly, for WOTT, it possesses an alternate behaviour; first increase then decreases possessing small amplitude but for $\theta_0 \ge 40^0$, it demonstrates an increasing behaviour as direction changes.

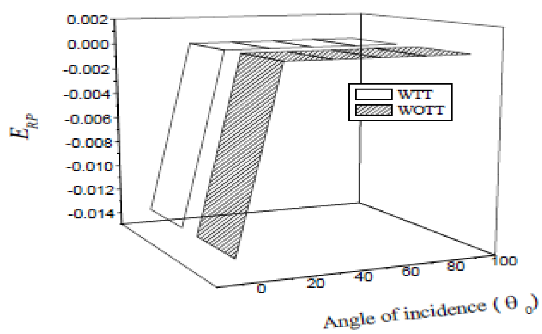

Fig.10
Profile of E_{RP} with θ_0 (P wave).

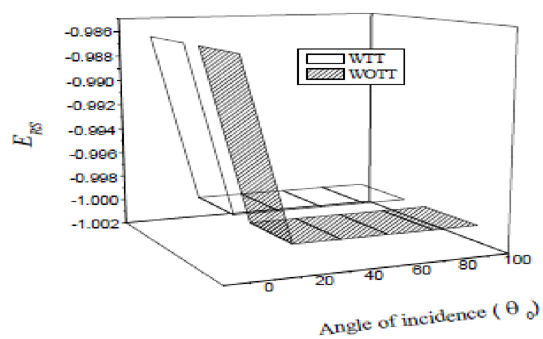

Fig.11
Profile of E_{RS} with θ_0 (SV wave).

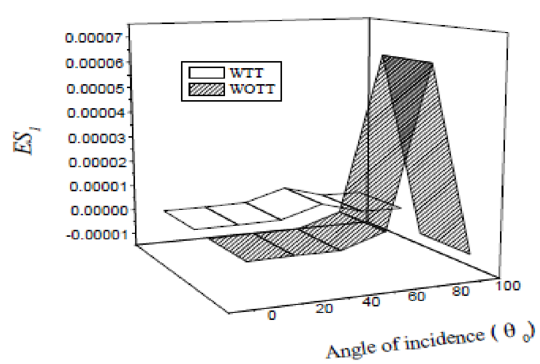

Fig.12
Profile of ES_1 with θ_0.

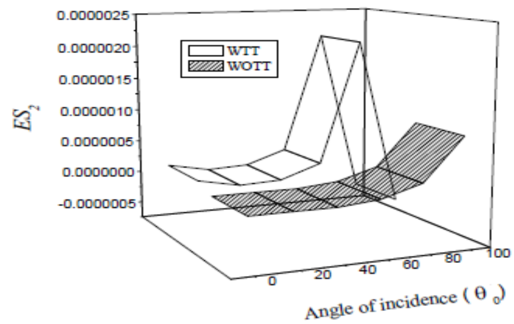

Fig.13
Profile of ES_2 with θ_0.

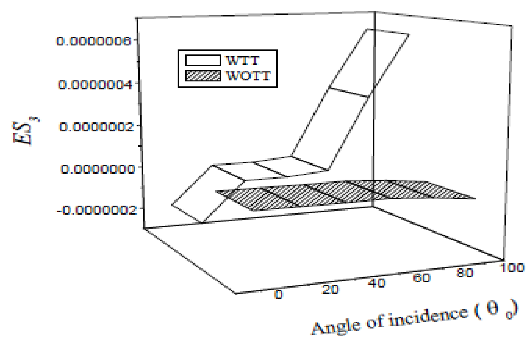

Fig.14
Profile of ES_3 with θ_0.

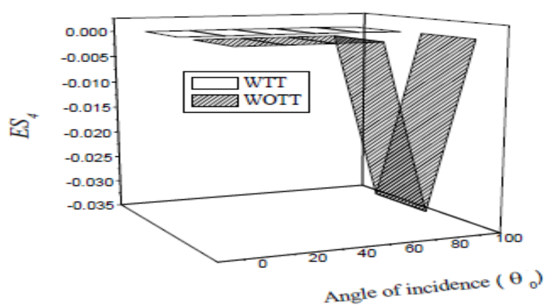

Fig.15
Profile of ES_4 with θ_0.

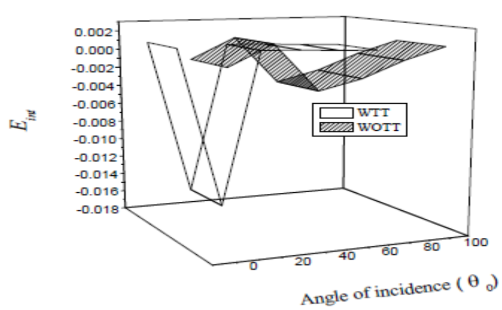

Fig.16
Profile of E_{int} with θ_0.

6 CONCLUSIONS

The mathematical study is to discuss the wave phenomenon of elastic waves at an interface of ES and OPS. This phenomenon is studied with the consideration of two-temperature. The energy ratios of different reflected and transmitted waves are obtained by using the amplitude ratios and these ratios are discussed and represented graphically to show the effect of two-temperature. The following observations are made from the above study.

- Amplitude ratios and energy ratios are impacted by the frequency, angle of incidence, two-temperature parameter and physical properties of the material. The nature of this dependence is different for distinct waves.
- Numerical results reveal that the reflection and transmission coefficient along are influenced significantly by the two-temperature parameter.
- It is found that sum of these energy ratios is approximately unity at each angle of incidence. This shows that there is no dissipation of energy during reflection and transmission phenomenon.
- It is observed that due to the effect of two-temperature parameter the larger part of energy goes into transmitted QT wave and some into reflected wave and interaction energy of the waves.
- For WTT model, for the incident P wave, only the energy ratios E_{RS} , ES_3 tend to increase as angle of incidence increases whereas for SV wave to be the incident wave, the energy ratios E_{RS} , ES_3 , E_{int} tend to increase with respect to angle of incidence.
- Principle of conservation of energy has been verified.

APPENDIX A

$$t_{11}=T_0(i\omega-\omega^2\tau_0),\ t_{12}=\frac{\alpha_{11}T_0}{e_{31}},\ t_{13}=-\frac{i\rho c_1^2}{\omega c},\ t_{14}=1+\omega^2\frac{a_{11}}{c^2},\ t_{15}=\omega^2 a_{33},\ t_{16}=-\frac{i\rho c_1^2\alpha_{33}}{\omega\alpha_{11}},$$

$$t_{17}=-\frac{\rho}{\alpha_{11}},\ t_{18}=t_{17}\omega_1\omega^2,\ t_{19}=-t_{11}c_1^2 r,\text{where } r=\frac{\rho C_e}{T_0},\ t_{20}=\frac{i\rho c_1^2\tau_3}{\omega\alpha_{11}}.$$

$$x_{11}=\frac{c_{11}}{c^2}-\rho c_1^2,\ x_{12}=\frac{(c_{13}+c_{55})}{c}=x_{16},\ x_{13}=\frac{(e_{31}+e_{15})}{c}t_{12},\ x_{14}=t_{13}t_{14},\ x_{15}=t_{13}t_{15},x_{17}=\frac{c_{55}}{c^2}-\rho c_1^2,$$

$$x_{18}=\frac{t_{12}e_{15}}{c^2},\ \ x_{19}=t_{12}e_{33},\ x_{20}=t_{14}t_{16},\ x_{21}=t_{15}t_{16},x_{22}=\frac{i\omega\alpha_{11}t_{11}}{c},x_{23}=i\omega\alpha_{33}t_{11},x_{24}=-i\omega\tau_3 t_{12}t_{11},$$

$$x_{25}=\frac{t_{18}K_{11}}{c^2},x_{26}=t_{18}K_{33},\ x_{27}=t_{14}t_{19},\ x_{28}=t_{15}t_{19},\ \ x_{29}=x_{25}+x_{27},x_{30}=x_{26}+x_{28},x_{31}=\frac{\left(e_{31}+e_{15}\right)}{c},$$

$$x_{32}=\frac{e_{15}}{c^2},x_{33}=\frac{-t_{12}\xi_{11}}{c^2},x_{34}=-t_{12}\xi_{33},\ \ x_{35}=t_{14}t_{20},\ x_{36}=t_{15}t_{20}.$$

$$b_{11}=x_{17}x_{33}-x_{18}x_{32},b_{12}=c_{33}x_{33}+x_{17}x_{34},b_{13}=-\left(x_{19}x_{32}+x_{18}e_{33}\right),b_{14}=b_{12}+b_{13},b_{15}=c_{33}x_{34}-x_{19}e_{33},$$

$$b_{16}=x_{12}x_{33}-x_{18}x_{31},b_{17}=x_{12}x_{34}-x_{19}x_{31},b_{18}=x_{12}x_{32}-x_{17}x_{31},b_{19}=x_{12}e_{33}-c_{33}x_{31},$$

$$b_{20}=c_{55}b_{11}+x_{11}b_{14}-x_{12}b_{16}+x_{13}b_{18},b_{21}=c_{55}b_{14}+x_{11}b_{15}-x_{12}b_{17}+x_{13}b_{19}$$

$$m_{11}=c_{55}x_{26}b_{15},\ m_{12}=b_{15}x_{25}c_{55}+x_{26}b_{21},\ m_{13}=b_{21}x_{25}+b_{20}x_{26},\ m_{14}=b_{20}x_{25}+x_{26}x_{11}b_{11},m_{15}=x_{11}x_{25}b_{11}.$$

APPENDIX B

$$D_{1i}=-\frac{c_{13}}{c}-c_{33}q_iW_i-\frac{\alpha_{11}T_0e_{33}}{e_{31}}q_i\Phi_i-\frac{\alpha_{33}\rho c_1^2}{i\omega\alpha_{11}}\left(1+\omega^2\frac{a_{11}}{c^2}+\omega^2a_{33}q_i^2\right)\Theta_i,$$

$$D_{2i}=-c_{55}\left(\frac{W_i}{c}+q_i\right)+\frac{e_{15}c_1\alpha_{11}T_0}{ce_{31}\omega_1}\Phi_i,\ D_{3i}=1,D_{4i}=W_i,\ D_{5i}=\left(1+\omega^2\frac{a_{11}}{c^2}+\omega^2a_{33}q_i^2\right)q_i\Theta_i,$$

$$D_{6i}=-\frac{e_{31}}{c}-e_{33}q_iW_i+\frac{\xi_{33}T_0\alpha_{11}}{e_{31}}q_i\Phi_i+\frac{\tau_3\rho c_1^2}{i\omega\alpha_{11}}\left(1+\omega^2\frac{a_{11}}{c^2}+\omega^2a_{33}q_i^2\right)\Theta_i,\quad (i=1,2,3,4).$$

For incident P wave

$$D_{15} = -i\,\omega\rho^e c_1^2\left(1-\frac{2\beta^{e^2}\sin^2\theta_0}{\alpha^{e^2}}\right),\ D_{16} = i\,\omega\rho^e c_1^2\sin 2\theta_2\,,\ D_{25} = \frac{i\,\omega\beta^{e^2}\rho^e c_1^2\sin 2\theta_0}{\alpha^{e^2}},$$

$$D_{26} = i\,\omega\rho^e c_1^2\cos 2\theta_2,\ D_{35} = \frac{i\,\omega c_1\sin\theta_0}{\alpha^e},\ D_{36} = \frac{i\,\omega c_1\cos\theta_2}{\beta^e},\ D_{45} = -\frac{i\,\omega c_1\cos\theta_0}{\alpha^e},\ D_{46} = \frac{i\,\omega c_1\sin\theta_2}{\beta^e},$$

$$X_i = \frac{U_i}{A_0^e},(i=1,2,3,4)\ ,\ X_5^e = \frac{A_1^e}{A_0^e},X_6^e = \frac{B_1^e}{A_0^e},\ N_1 = -D_{15},\ N_2 = D_{25},\ N_3 = -D_{35},\ N_4 = D_{45}.$$

For incident SV wave

$$D_{15} = -i\,\omega\rho^e c_1^2\left(1-\frac{2\beta^{e^2}\sin^2\theta_1}{\alpha^{e^2}}\right),\ D_{16} = i\,\omega\rho^e c_1^2\sin 2\theta_0\,,\ D_{25} = \frac{i\,\omega\beta^{e^2}\rho^e c_1^2\sin 2\theta_1}{\alpha^{e^2}},$$

$$D_{26} = i\,\omega\rho^e c_1^2\cos 2\theta_0,\ D_{35} = \frac{i\,\omega c_1\sin\theta_1}{\alpha^e},\ D_{36} = \frac{i\,\omega c_1\cos\theta_0}{\beta^e},\ D_{45} = -\frac{i\,\omega c_1\cos\theta_1}{\alpha^e},\ D_{46} = \frac{i\,\omega c_1\sin\theta_0}{\beta^e},$$

$$X_i = \frac{U_i}{B_0^e},(i=1,2,3,4)\ ,\ X_5^e = \frac{A_1^e}{B_0^e},X_6^e = \frac{B_1^e}{B_0^e},\ N_1 = D_{16},\ N_2 = -D_{26},\ N_3 = D_{36},\ N_4 = -D_{46}.$$

REFERENCES

[1] Chen P. J., Gurtin M. E., 1968, On a theory of heat conduction involving two temperatures, *The Zeitschrift für Angewandte Mathematik und Physik* **19**: 614-627.

[2] Chen P. J., Gurtin M. E., Williams W. O., 1968, A note on non-simple heat conduction, *The Zeitschrift für Angewandte Mathematik und Physik* **19**: 969-970.

[3] Chen P. J., Gurtin M. E., Williams W. O., 1969, On the thermodynamics of non-simple elastic materials with two temperatures, *The Zeitschrift für Angewandte Mathematik und Physik* **20**(1): 107-112.

[4] Sharma K., Marin M., 2013, Effect of distinct conductive and thermodynamic temperatures on the reflection of plane waves in micropolar elastic half-space, *Applied Mathematics Physics* **75**(2): 121-32.

[5] Kumar R., Vashishth A. K., Ghangas S., 2018, Waves in anisotropic thermoelastic medium with phase lag, two-temperature and void, *Materials Physics and Mechanics* **35**: 126-138.

[6] Mindlin R.D., 1974, Equation of high frequency of thermopiezoelectric crystals plates, *International Journal of Solids and Structures* **10**: 625-637.

[7] Nowacki W., 1978, Some general theorems of thermo-piezoelectricity, *Journal of Thermal Stresses* **1**: 171-182.

[8] Nowacki W., 1979, *Foundation of Linear Piezoelectricity*, Interactions in Elastic Solids, Springer, Wein.

[9] Vashishth A.K., Sukhija H., 2014, Inhomogeneous waves at the boundary of an anisotropic piezo-thermoelastic medium, *Acta Mechanica* **225**: 3325-3338.

[10] Vashishth A.K., Sukhija H., 2015, Reflection and transmission of plane waves from fluid piezothermoelastic solid interface, *Applied Mathematics and Mechanics* **36**(1): 11-36.

[11] Vashishth A.K., Sukhija H., 2017, Inhomogeneous waves in porous piezo-thermoelastic solids, *Acta Mechanica* **228**: 1891-1907.

[12] Kumar R., Sharma P., 2017, Effect of fractional order on energy ratios at the boundary surface of elastic-piezothermoelastic media, *Coupled Systems Mechanics* **6**(2):157-174.

[13] Marin M., Ochsner A., 2017, An initial boundary value problem for modelling a piezoelectric dipolar body, *Continuum Mechanics and Thermodynamics* **32**(2): 267-78.

[14] Sharma M.D., 2018, Reflection–refraction of attenuated waves at the interface between a thermo-poroelastic medium and a thermoelastic medium, *Waves in Random and Complex Media* **28**(3): 570-587.

[15] Kumar R., Sharma P., 2020, Basic theorems and wave propagation in a piezothermoelastic medium with dual phase lag, *Indian Journal of Physics* **94**: 1975-1992.

[16] Bassiouny E., Youssef H. M., 2008, Two-temperature generalised thermopiezoelasticity of finite rod subjected to different types of thermal loadings, *Journal of Thermal Stresses* **31**(1): 233-245.

[17] Ezzat M.A., El-Karamany A.S., Awad E. S., 2010, On the coupled theory of thermo-piezoelectric/ piezomagnetic materials with two-temperature, *Canadian Journal of Physics* **88**(5): 307-315.

[18] Tzou H. S., Bao Y., 1995, A theory on anisotropic piezothermoelastic shell laminates with sensor/actuator applications, *Journal of Sound and Vibration* **184**(3): 453-473.
[19] Bullen, K. E., 1963, *An Introduction to the Theory of Seismology*, Cambridge University Press, England.